Bio-Medical Materials and Engineering 24 (2014) 2725–2732
DOI 10.3233/BME-141090
IOS Press


# Dielectric properties of human liver from 10Hz to 100MHz: normal liver, hepatocellular carcinoma, hepatic fibrosis and liver hemangioma[1]

Hang Wang[a], Yong He[b], Min Yang[b], Qingguo Yan[c], Fusheng You[a], Feng Fu[a], Ting Wang[a], Xuyang Huo[a], Xiuzhen Dong[a,*] and Xuetao Shi[a,*]
[a]*Department of Biomedical Engineering, Fourth Military Medical University, No. 169 Changle West Road, 710032, Xi'an, China*
[b]*Xijing Hospital, Fourth Military Medical University, No. 169 Changle West Road, 710032, Xi'an, China*
[c]*Department of Pathology, Fourth Military Medical University, No. 169 Changle West Road, 710032, Xi'an, China*

**Abstract.** The dielectric properties of human liver were determined by characterization of tissue absorption and coupling of electromagnetic energy in the electromagnetic field. In this study the ex-vivo dielectric properties of human hepatocellular carcinoma (well and moderately differentiated), liver hemangioma, hepatic fibrosis (stages S1 and S2), and normal liver tissue were measured and analyzed over the frequency range of 10 Hz to 100 MHz. The dielectric properties over the frequency range can reflect tissue information including biological macromolecules, vesicles, and cellular membrane; these information aids in distinguishing different physiological states and lesions. The ex-vivo conductivity, permittivity, resistivity, as well as the characteristic parameters between the lesions and normal liver were analyzed and their differences were also verified. The data can contribute to developing bioelectric applications for tissue diagnostics and creating more accurate computer models for medical applications.

Keywords: Dielectric property, characteristic parameters, liver cancer, hepatic fibrosis

[1]Hang Wang and Yong He are thought to have equal contributions. Moreover, the authors declare that there is no conflict of interests regarding the publication of this paper.

[*]Corresponding authors: Xuetao Shi, Department of Biomedical Engineering, Fourth Military Medical University, No. 169 Changle West Road, 710032, Xi'an, China. Tel.: +8602984774848; Fax: +8602984774848; E-mail: shixuetao@fmmu.edu.cn.

Xiuzhen Dong, Department of Biomedical Engineering, Fourth Military Medical University, No. 169 Changle West Road, 710032, Xi'an, China. Tel.: +8602984776397; Fax: +8602984776397; E-mail: dongxiuzhen@fmmu.edu.cn.

## 1. Introduction

The dielectric properties of biological tissues exhibit current conduction (conductivity) and storage abilities to electric charges (relative permittivity). The properties are closely related to cell density, arrangement mode, membrane capacitance, and conductivity in the cytoplasm or cells in tissues [1,2]. Various tissues may thus possess dielectric properties at different pathological and physiological states.

The dielectric properties of human liver this study obtained could be useful and meaningful. Several new cancer treatments require knowledge of the dielectric properties of liver tissue, such as radiofrequency (RF) thermal ablation. A previous study has shown that accurate knowledge regarding the conductivities of different tissue types (normal and tumor) is essential in creating accurate computer models of RF ablation [3]. Studies on the dielectric properties between human normal liver and tumor tissues have been reported [4–6]. However, the current works are unclassified for types of tumor tissues. The causes of tumors are different, which yield different dielectric properties; these crucial data remain sparse or missing. Any additional data on measured diseased tissues are necessary. In this paper, diseased tissues are referred to as hepatic fibrosis, hepatocellular carcinoma (HCC), and liver hemangioma. HCC morbidity and mortality are the fifth and the third among all cancers worldwide [1], respectively. Liver hemangioma is a common and benign liver tumor.

The dielectric properties of human living normal liver, HCC, hepatic fibrosis, and liver hemangioma were systematically measured within 10 Hz to 100 MHz to obtain the sensitive indicators and the distinguishing features of these tissues by dielectric properties. The obtained data could contribute to developing bioelectric applications for tissue diagnostics and liver treatment using electrical fields (e.g., RF ablation).

## 2. Materials and methods

### *2.1. Sample source*

The research was approved by the Medical Ethics Committee of the Fourth Military Medical University (Approval No. FMMU-E-III-001(1)). A total of 132 cases of liver tissue samples from 116 patients with hepatectomy were obtained in the General Surgery Operating Room of Xijing Hospital. The average age of the patients was 49±12 years. Following the dielectric measurement, all tissue samples were processed with pathological HE staining by the Pathology Department. The tissue types were then identified.

Among 132 reported cases, 26 of which have normal liver tissues, 31 of which exhibit HCC (well and moderately differentiated HCC), 28 of which have liver hemangioma, and 47 of which manifest hepatic fibrosis. Hepatitis was often graded (necro-inflammation) and staged (fibrosis) using the Scheuer system [7]. Four stages of fibrosis (S1 to S4) were used to clarify the development stages of liver injuries [8]. In this study, hepatic fibrosis belonged to stages S1 and S2.

### *2.2. Measurement system*

The measurement frequency varied from 10 Hz to 100 MHz; the impedance analyzer mainly included Solartron 1260 (Schlumberger, UK) and Agilent 4294A (Agilent Technologies, USA). Solartron 1260 was mainly used to measure the impedance from 10 Hz to 1 MHz. The 4-electrode

method [9] was used at this frenquency range to eliminate polarization effects of the electrodes. While Agilent 4294A was mainly used to measure the impedance from 10 kHz to 100 MHz. The 2-electrode method [10] was applied to reduce the effects of stray capacitance and inductance. The equipment adopted the logarithmic scanning method that uses ten points for every 10-fold increase in frequency.

Measurements were controlled strictly over the sample ex vivo time (30 min after separation) and the environment condition (37°C and 90% relative humidity). The result of each sample was the mean value of three individual measurements. Before any dielectric measurements were made, the system was calibrated by using saline solution with different concentrations.

### *2.3. Calculation of the dielectric properties of biological tissues*

The data obtained by the equipment included the real part *Re* and the imaginary part *Im*. The conductivity ($\sigma$) and permittivity of tissues ($\varepsilon_r$) can be written as

$$\sigma = \frac{\mathrm{Re}\cdot L}{(\mathrm{Re}^2+\mathrm{Im}^2)\cdot S} \tag{1}$$

$$\varepsilon_r = -\frac{\mathrm{Im}\cdot L}{2\pi\cdot f_0\cdot\varepsilon_0\cdot S\cdot\left(\mathrm{Re}^2+\mathrm{Im}^2\right)} \tag{2}$$

where $\varepsilon_0$ represents the vacuum permittivity, $S$ is the cross-sectional area of the sample, and $L$ is the effective sample length.

### *2.4. The Cole–Cole model and calculation of characteristic parameters*

Cole et al. showed that the dielectric properties of biological tissues meet the Cole equation [11]:

$$Z(f) = R_\infty + (R_0 - R_\infty)/\left[1+(j f/f_c)^\alpha\right] \tag{3}$$

where $R_\infty$ is the limit value of impedance at a high frequency, $R_0$ is the impedance at DC, $f_C$ is the characteristic frequency of the relaxation, $\alpha$ is the dispersion angle of the relaxation ($0<\alpha<1$), and $j$ is the unit of the imaginary part by which $j=\sqrt{-1}$.

Schwan [12] stated that different dispersions can be found in biological tissues, including α- (from 10 Hz to ~$10^3$ Hz), β- (from $10^3$ Hz to <$10^7$ Hz), δ- (<$10^{10}$ Hz), and γ-dispersion (>$10^{10}$ Hz). The dispersions correspond to different relaxation phenomena and are distributed in various frequency ranges [13]. To accurately characterize the different tissues by limited parameters, the Cole equation was extended for several dispersions and obtained the general equation of the dielectric properties of biological tissues given as

$$Z(f) = R_\infty + \sum_{i=1}^{n} \Delta R_i \Big/ \left[1 + (j f / f_{ci})^{\alpha i}\right] \quad (4)$$

Where $i$ represents the existing dispersion of the tissue by which one or more dispersions exist (Eq. (4)); $\Delta R_i$ is the incremental impedance of the dispersion. Thus, the characterization of the dielectric properties of the related tissues was converted into the solutions of $R_\infty$, $\Delta R_i$, $\alpha_i$, and $f_{ci}$. Each category of the characteristic parameters was processed using one-way ANOVA to determine the indicators suitable for distinguishing normal liver tissues, HCC, liver hemangioma, and fibrosis. SPSS 13.0 was used for comparisons.

## 3. Results

### *3.1. Differences of dielectric properties among four-tissue types*

The conductivity, permittivity, and resistivity were applied to characterize and analyze the dielectric properties of the samples. Figure 1A reveals that the conductivities of tissues from the liver with hemangioma were two to three times higher than the rest of the tissues. Below 1 MHz, the conductivity of the hepatic fibrosis was the largest followed by tissues from normal liver and HCC. The differences among the three tissues gradually decreased with increasing frequency. Changes in permittivity of the four types of liver tissues were similar (Figure 1B); the permittivity rapidly decreased below 1 kHz. After a transient and stable change, the permittivity rapidly decreased again after 10 kHz. At low frequencies, the permittivity of cavernous hemangioma was the largest followed by tissues from fibrosis, normal liver, and HCC.

The real parts of the resistivity of the tissues from normal liver, HCC, hepatic fibrosis, and liver hemangioma under 1 kHz were approximately 1025, 1455, 746, and 381 Ω·cm, respectively (Figure 1C). At high frequencies, the real parts of the resistivity of tissues from normal liver, HCC, and hepatic fibrosis were similar; the value for tissues from liver hemangioma was lower than that from the other tissues. Two peaks of the imaginary part of resistivity appeared from 10 Hz to 100 MHz (two square frames in Figure 1D). The peak means the minimum of the imaginary part of resistivity in the certain frequency range. The frequency of the peak is the characteristic frequency. The first characteristic frequency appeared from 10 kHz to 1 MHz; the second characteristic frequency appeared from 10 MHz to 100 MHz, and the imaginary part of the resistivity of the four tissues were concentrated between −50 and −100 Ω·cm.

### *3.2. Mathematical modeling and statistical analysis of the model parameters*

Figure 1E reveals that two dispersions exist from 10 Hz to 100 MHz. Accordingly, Table 1 shows the characteristic parameters of each tissue. $R_0$ and $\Delta R_1$ can completely distinguish the tissues from normal liver, HCC, hepatic fibrosis, and cavernous hemangioma ($p < 0.05$); $f_{c1}$ cannot distinguish the tissues from normal liver and HCC ($p = 0.079$). $\alpha_1$ cannot likewise differentiate the tissues from normal liver and fibrosis ($p = 0.976$); $f_{c2}$, $\alpha_2$, and $\Delta R_2$ cannot distinguish the tissues from normal liver, fibrosis, and HCC ($p > 0.05$). However, $f_{c2}$, $\alpha_2$, and $\Delta R_2$ of the tissues from cavernous hemangioma exhibited statistically significant differences from the liver tissues from other states ($p < 0.05$).

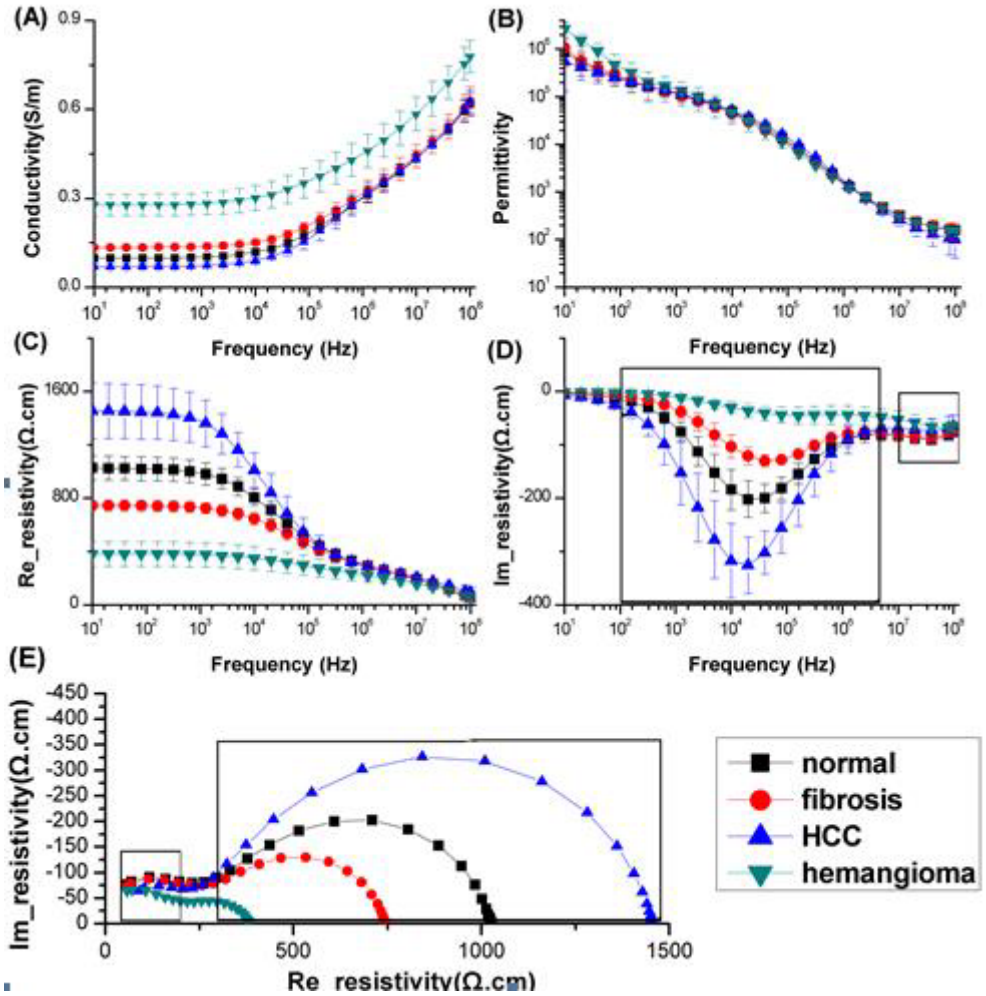


Fig. 1. The dielectric properties of the tissues from normal liver, HCC, fibrosis, and cavernous hemangioma. (A) Conductivity; (B) permittivity; (C, D) average real and imaginary parts of resistivity ρ of the four liver tissues; (E) Cole–Cole curves of the liver tissues.

Although $f_{c1}$ cannot completely distinguish the four types of liver tissues; the imaginary part of the resistivity of these tissues peaked when the frequency was at $f_{c1}$ of –202±34, −326±53, −130±11, and –45±16 Ω·cm in tissues from normal liver, HCC, hepatic fibrosis, and cavernous hemangioma (Figure 1D), respectively. One-way ANOVA was used for statistical analysis ($p<0.001$). The four kinds of tissues revealed statistical differences.

### *3.3. Morphological characteristics of the liver tissues*

Figures 2a and 2b respectively present the normal liver and the pathological section of HCC. The cell density of HCC increased and exhibited irregular, small beam-like acinus or pseudoglandular structures. The results indicated that the conductivity of HCC tissues at low frequencies was lower than those of normal liver tissues, which was attributed to the effect on the conductivity and

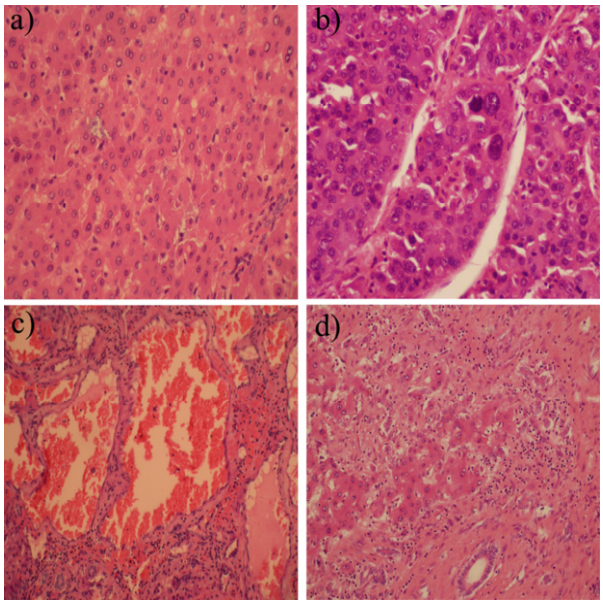


Fig. 2. Pathological section of tissues from (a) normal liver, (b) HCC, (c) liver hemangioma, and (d) hepatic fibrosis

Table 1

Characteristic parameters of the four types of liver tissues (mean±SD)

| | $R_0(\Omega)$ | $f_{c1}$(kHz) | $\alpha_1$ | $\Delta R_1(\Omega)$ | $f_{c2}$(MHz) | $\alpha_2$ | $\Delta R_2(\Omega)$ |
|---|---|---|---|---|---|---|---|
| (1) normal liver | 1057±100 | 39.7±16.9 | 0.56±0.04 | 836±86 | 39.7±4.8 | 0.80±0.03 | 220±19 |
| (2)hepatic fibrosis | 760±38 | 77.1±31.2 | 0.55±0.03 | 548±35 | 39.4±9.8 | 0.83±0.03 | 212±27 |
| (3)HCC | 1480±212 | 20.2±10.3 | 0.64±0.01 | 1226±199 | 36.5±4.8 | 0.79±0.03 | 238±16 |
| (4)hepatic hemangioma | 389±95 | 235.4±105.6 | 0.45±0.02 | 253±64 | 60.0±9.5 | 0.85±0.03 | 141±9 |
| difference between groups (p) | 0 | 0 | 0 | 0 | 0.001 | 0.003 | 0 |
| P12 † | 0 | 0.040 | 0.976 | 0 | 1.000 | 0.057 | 1.000 |
| P13 | 0.039 | 0.079 | 0 | 0.043 | 0.771 | 1.000 | 0.736 |
| P14 | 0 | 0.013 | 0 | 0 | 0.004 | 0.001 | 0 |
| P23 | 0.006 | 0.003 | 0 | 0.006 | 0.979 | 0.066 | 0.174 |
| P24 | 0 | 0.033 | 0 | 0 | 0.007 | 0.786 | 0 |
| P34 | 0 | 0.008 | 0 | 0.001 | 0.002 | 0.003 | 0 |

*Note:* † P12 indicates the p value between the tissues from (1) normal liver and (2) hepatic fibrosis; P13 is the p value between the tissues from (1) normal liver and (3) HCC, and so on.

permittivity from the extracellular fluid. The increased cell density of the cancer tissues was accompanied by partial restructuring and steatosis, which yielded lower extracellular fluid and smaller conductivity than those of normal liver tissues.

Figure 2c shows that the cavernous hemangioma was alveolate and filled with different sizes of capsular blood sinuses. The walls of the sinuses were covered with a layer of endothelial cells. The structure of internal liver hemangioma was destroyed. Thus, the dielectric properties of the cavernous hemangioma exhibited significant differences from the other liver tissues. Figure 2d indicates the pathological section of hepatic fibrosis. The portal area was expanded with fibrosis; fibrous septa were

formed, and the lobular structure was retained. Given that S1 and S2 belonged to light and medium fibrosis, the structures of the hepatic lobules were preserved. The results revealed that the conductivity and permittivity of tissues from hepatic fibrosis were slightly higher than those of normal liver tissues, which was attributed to the fibrocytes in the tissues.

## 4. Discussion

This study first integrated the pathological types to measure systematically the dielectric properties of living tissues form human normal liver, HCC, hepatic fibrosis, and liver hemangioma under strict specifications over the entire frequency range (10 Hz to 100 MHz).

Figure 1E shows that all samples had two dispersions from 10 Hz to 100 MHz. The two dispersions of the sample dielectric properties may corresponded to $\beta$-and $\delta$-dispersions [14]. $\beta$-dispersion was mainly associated with the cell structure of the tissues and the polarization of the cell membrane. Analysis of the characteristic parameters ($f_{c1}$, $\alpha_1$, and $\Delta R_1$; Table 1) showed that significant differences existed in $\beta$-dispersion among the four-tissue types. In contrast to normal liver tissues, the cellular morphology and arrangement mode of the lesions showed different levels and types of degeneration, which altered the original structure or integrity of the cell membrane. $\delta$-dispersion was associated with the polarization of intracellular proteins or other macromolecular compounds [5,14,15]. Analyses of the characteristic parameters ($f_{c2}$, $\alpha_2$, and $\Delta R_2$; Table 1) indicated that the fibrosis and cancerous tissues were differentiated from normal liver tissues; thus, changes in the contents of the corresponding proteins or other macromolecular compounds were insignificant.

The results of the dielectric properties between human normal liver tissues and malignancy tissues showed significant differences based on previous studies [4–6,16]. The results were attributed to the inconsistent measurements from different research groups because of the uncertainty in tumor type, stage, and occurrence site. In this paper, the malignancy referred to the HCC (well and moderately differentiated), hepatic fibrosis (belonged to stages S1 and S2), and cavernous hemangioma. The occurrence sites of cancers were also strictly controlled. Detailed classification and accurate measurements yielded increased significance of clinical applications.

Furthermore, ex-vivo liver tissues were placed in the measurement cell [17,18] to ensure the consistency of the sample sizes and reduce the error caused by the different operational procedures. Only the strict control of the possible influencing factors can increase data accuracy. The obtained data could be comparable if the experiment used the same measurement method.

## 5. Conclusion

The dielectric properties could effectively distinguish the tissues from HCC, hepatic fibrosis, liver hemangioma, and normal liver; the results could serve as the basis for future studies. The obtained data could contribute to developing bioelectric applications for tissue diagnostics and liver treatment using electrical fields. Additional clinical samples could be collected in the future studies to subdivide the tissue types and comprehensively compare the dielectric properties of different human liver tissues. This approach will effectively prepare the accurate differentiation of the lesion types and stages of liver tissues.

## Acknowledgement

This study was partially supported by the National Natural Science Foundation of China (Grant Nos. 50937005, 61071033 and 31100710), Military Foundation of China (CWS12J102) and the Key Technologies R&D Program of China (Grant Nos. 2012BAI19B01).

## References

[1] B. Rampone, B. Schiavone, A. Martino, C. Viviano and G. Confuorto, Current management strategy of hepatocellular carcinoma, World Journal of Gastroenterology **15** (2009), 3210–3216.
[2] K.R. Foster and H.P. Schwan, Dielectric properties of tissues and biological materials: A critical review, CRC Critical Reviews in Biomedical Engineering **17** (1989), 25–104.
[3] S.A. Solazzo, Z. Liu, S.M. Lobo, M. Ahmed, A.U. Hines-Peralta, R.E. Lenkinski and S.N. Goldberg, Radiofrequency Ablation: Importance of background tissue electrical conductivity-an agar phantom and computer modeling study, Radiology **236** (2005), 495–502.
[4] P. Stauffer, F. Rossetto, M. Prakash, D. Neuman and T. Lee, Phantom and animal tissues for modelling the electrical properties of human liver, International Journal of Hyperthermia **19** (2003), 89–101.
[5] D. Haemmerich, D.J. Schutt, A.S. Wright, J.G. Webster and D.M. Mahvi, Electrical conductivity measurement of excised human metastatic liver tumours before and after thermal ablation, Physiological Measurement **30** (2009), 459–466.
[6] S. Laufer, A. Ivorra, V.E. Reuter, B. Rubinsky and S.B. Solomon, Electrical impedance characterization of normal and cancerous human hepatic tissue, Physiological Measurement **31** (2010), 995–1009.
[7] P.J. Scheuer, Classification of chronic viral hepatitis: A need for reassessment, Journal of Hepatology **13** (1991) 372–374.
[8] J. Ludwig, The nomenclature of chronic active hepatitis: An obituary, Gastroenterology **105** (1993), 274–278.
[9] R. Agarwal and V.R. Singh, Dielectric properties of kidney stones as electro-ceramics, Bio-Medical Materials and Engineering **1** (1991), 155–158.
[10] H.P. Schwan, Determination of biological impedances, Physical Techniques in Biological Research: Electrophysiological Methods Pts. AB **6** (1963), 323–407.
[11] K.S. Cole and R.H. Cole, Dispersion and absorption in dielectrics, I. alternating current characteristics, The Journal of Chemical Physics **9** (1941), 341–351.
[12] H.P. Schwan, Electrical properties of tissue and cell suspensions, Advances in Biological and Medical Physics **5** (1957), 147-209.
[13] R. Pethig and D.B. Kell, The passive electrical properties of biological systems: Their significance in physiology, biophysics and biotechnology, Physics in Medicine and Biology **32** (1987), 933–970.
[14] M. Wolf, R. Gulich, P. Lunkenheimer and A. Loidl, Broadband dielectric spectroscopy on human blood, Biochimica et Biophysica Acta (BBA)-General Subjects **1810** (2011), 727–740.
[15] A.R. Portero, Development of a software application suite for electrical bioimpedance data analysis, M.S. Dissertation, Universitat Politècnica de Catalunya, 2010.
[16] A.P. O'Rourke, M. Lazebnik, J.M. Bertram, M.C. Converse, S.C. Hagness, J.G. Webster and D.M. Mahvi, Dielectric properties of human normal, malignant and cirrhotic liver tissue: In vivo and ex vivo measurements from 0.5 to 20 GHz using a precision open-ended coaxial probe, Physics in Medicine and Biology **52** (2007), 4707–4719.
[17] K. Folgero, Broad-band dielectric spectroscopy of low-permittivity fluids using one measurement cell, IEEE Transactions on Instrumentation and Measurement **47** (1998), 881–885.
[18] S. Comlekci, Induced dielectric-force-effect by 50 Hz strong electric field on living tissue, Bio-Medical Materials and Engineering **16** (2006), 363–367.